Asian Journal of Chemistry; Vol. 34, No. 9 (2022), 2205-2210

ASIAN JOURNAL OF CHEMISTRY

https://doi.org/10.14233/ajchem.2022.23765

Mechanism of Luminescence Enhancement in Eu^{3+} Activated Double Perovskite Phosphors $Bi_{2-x}Eu_xWO_6$ (x = 0-0.24) Prepared by Sol-Gel Method

K. Koteswara Rao*, and B. Nagamani Naidu

Department of Basic Science & Humanities, GMR Institute of Technology (Affliated to Jawaharlal Nehru Technological University Kakinada), Rajam-532127, India

*Corresponding author: E-mail: k.koteswararao@gmrit.edu.in

Received: 4 February 2022; *Accepted*: 14 April 2022; *Published online*: 19 August 2022; AJC-20910

A double perovskite structured series $Bi_{2-x}Eu_xWO_6$ (x = 0.03-0.24) was prepared by using simple citrate sol-gel method at 700 ºC for 5 h of sintering. The double perovskite structure and its lattice parameters were analyzed by the XRD technique and found to be pure orthorhombic phase. The concentrated sample of x = 0.12 exhibits more intensity than all other concentration in their emission spectra. Particle size, thickness of the particle, distance between particles and its surface morphology were identified by scanning electron microscopy. The size and distance between particles lies in between the range of 1-50 nm and 20-50 nm, respectively. In addition to this the absorption of light capacity for every sample was investigated through diffuse reflectance spectra method. All the samples of double perovskite structures exhibit a sharp cut-off of absorption light in the UV and visible regions of diffuse reflectance spectra. Predominantly, sample x = 0.12 shows very good charge transfer band in their excitation spectra that leads to more absorption of light correspondingly emits high intensity in emission spectra. All the samples of series emit main peaks in the range of 550-700 nm in their emission spectra. Out of all four main peaks, 614 nm peak represents the red phosphor with $^5D_0$–$^7F_2$ transition in the emission spectra. The prepared double perovskite structure compound CRI co-ordinates (0.6254, 0. 3739) are almost close to commercially available red phosphor *i.e.* Y_2O_2S (0.67, 0.33) as per NTSC. Hence, the prepared red phosphors can be used in order to display devices, luminescent materials and WLEDs.

Keywords: Sol-gel method, Luminescence, Bismuth tungstates, Red phosphors, Double perovskites.

INTRODUCTION

Currently, the researchers are paving usually more attention towards the white light-emitting diodes (WLEDs). The WLEDs have many advantages such as long life time, high luminescent efficiency and very low power consumption. Simultaneously, it has own feature of it's to function as eco-friendly in nature [1,2]. In this connection, the concerned WLEDs are generally made the using various strategies. Out of all strategies, the main synthetic routes are InGaN chip is coated on the yellow phosphor (YAG: Ce^{3+}), however this approach has some limitations such as colour rending index (CRI) is very low in the red region [3]. Second approach is the mixing of (red + green + blue) tricolour phosphor which is excited with near UV LED to produce white light emission [4]. But this approach has also some limitations. The usage of sulphur as well as oxy-sulphur derivatives, which are not ecofriendly in nature. Since, it emits harmful gases into the atmosphere [5-7]. The third strategy is UV-LED to excite three different phosphors (RGB) coated over the epoxy layers. Hence, one needs to formulate a new structured phosphor for producing high efficient WLEDs.

In this regard, it is recommended that the Eu^{3+} ion can be used as dopants in the red phosphors for improving the luminescence efficiency in the formation of strong and broad charge transfer band in the excitation spectra. The charge transfer band (CTB) is strong and broad the host crystal lattice absorbs more light energy and it transfers to rare earth activator ion Eu^{3+}, which leads to high intensity emission spectra [8].

However, the WLEDs are mostly prepared by using solid-state method. But this method faces many limitations for example, (i) requisition of high calcination temperature, (ii) grinding of powder for long time, and (iii) the physical state of fine powder is non-homogeneity. On account of limitation, the prepared WLEDs are directly affected in various ways like

as such high calcination temperature causes the damage surface of the powder that leads to crystal defects. Finally, the above mentioned reasons cause decrease the phosphor luminescence efficiency. As a result, to avoid all the above said drawbacks, one should proceed with sol-gel method. The sol-gel method has many advantages as such the preparation of phosphor at ease, economically cheap, high quality and predominantly high homogeneity with tiny particles. Moreover, this method requires low temperature, in comparison with solid state method.

Tungstate's contain of double perovskite structures, which are mostly used in the applications of both phosphors materials and scintillators [9,10]. Generally, tungstate acts like a self-activated luminescent materials due to wide range of intrinsic emission band [11-13]. Hence, intrinsic emission transitions are formed due to annihilation of self-trapped excitation with UV light. However, the materials are excited with UV light, which have high stoke shift is about 16,000 cm. In case of tungstate's containing double parton scatterings (DPS), the stoke shift is very low. Hence, one can use as applications of WLEDs [14].

Bismuth is considered as green main group element due to its non-carcenogenic nature and non-toxic nature [15]. Moreover, Bi^{3+} ion shows both strong absorption band in UV region and emits a broad band emission extending from UV to red spectral range due to $^3P_{1,0}$–$^1S_{1,0}$ transition [16]. In addition to this, the starting materials are also accessible for stoichiometry calculation. In this work, the red phosphor $Bi_{2-x}Eu_xWO_6$ (x = 0-0.24) was prepared with sol-gel method. Moreover, its crystal structure, surface morphology, luminescence efficiency and colour absorption regions were also investigated.

EXPERIMENTAL

Synthesis: $Bi_{2-x}Eu_xWO_6$ (x = 0.12) compound was prepared with simple citrate sol-gel method at 700 ºC for 5 h of sintering. In brief, weighed 1.4212 g of Bi_2O_3, 0.1528 g of Eu_2O_3, 1.8083 g of H_2WO_4, 3.146 g of citric acid (stoichiometric ratio of total cations to citric acid as 1.0:1.5) and transferred to 500 mL glass beaker followed by the addition of the distilled water to get a clear solution. If any sample is not dissolved in distilled water, added either nitric acid or liquid ammonia. After that, the solution should maintain its pH in around 6-7 by adding required amount of either acid or base to the solution. The total quantity of the solution should not exceed 300 mL. Place the glass beaker on the magnetic stirrer, which contains two nobs for simultaneous heating as well as stirring. Left the solution on the magnetic stirrer for 6-8 h at 100 ºC for both simultaneous heating and stirring. Then, before the formation of a grey gel liquid, added 1.5 mL of ethane diol or ethylene glycol dropwise to the solution mixture. After 8 h of simultaneous heating and stirring, it produces a grey gel sample. Then, the gel substance was burned in an electric burner for 15-20 min, which turns into the grey powder form. This powder form was grinded in mortar pestle up to fine powder state. Finally, fine powder was annealed at various temperatures *viz*. 500 ºC, 600 ºC, 700 ºC for 5 h in a muffle furnace.

Characterization: XRD patterns were recorded by using X-ray diffractrometer (Phillips PW 1830) with Cu$K\alpha$ radiation (K = 0.15406 Å) at 36 kV tube voltage and 20 mA tube current. On the other hand, the angles (2θ) values were recorded for every structure in between 10º-90º with 0.02 scanning speed and 4º/min scanning rate, respectively. The light absorbance capacity was measured with diffuse reflectance spectra (Perkin Elmer UV Win lab 6.2.0.0741 λ_{35} 1.27). Surface morphology, size and distance between particles were measured with FESEM (Oxford instruments). Excitation and emission spectra were recorded by using PL data (FP8300, Serial number D046261450). CRI coordinates were measured by using Osram Sylvania color calculator.

RESULTS AND DISCUSSION

Crystallinity and phase purity: The double perovskite structured samples have been prepared by sol-gel method, at various temperatures *i.e*., 500, 600, 700 ºC for 5 h of each series. However, XRD technique can be used in order to find the structural characterization of these double perovskite structured compounds. When the above samples which are synthesized at 500 and 600 ºC for 5 h, exhibits impurities as well as double perovskite phases through XRD pattern. As a result in order to form purified, perfect, well matched crystal structure, one has to be annealed the sample at 700 ºC for 5 h. Annealing beyond 700 ºC for 5 h, it was observed of its partial melting of the samples. During the process of observation, one should fixed 700 ºC for 5 h is the optimum temperature for the prep-aration of red phosphor compounds. Finally, to identify the structural and optical characterization, the samples which were annealing at 700 ºC for 5 h. The sample structures are named through Nakmuta program [17]. Hence, the samples of XRD pattern and its structure shown in Fig. 1.

The samples annealed at 700 ºC/5 h (Fig. 1b) showed good phase purity and high crystallinity having pure orthorhombic $Bi_{2-x}Eu_xWO_6$ type crystal structure (JCPDS No.73-1126). Space group: B2ab, Space group number: 41 [18].

Diffuse reflectance spectroscopy: From Fig. 2, it is observed that the DRS for the double perovskite structures which is prepared at 700 ºC for 5 h and clearly showed that the absorbance capacity of phosphor appear in two regions. The first region of absorbance band ranging from 250-380 nm due to oxygen–Mo charge transfer transition [19]. The second region ranging from 420-480 nm, which is weak absorption band, due to *f-f* transition of Eu^{3+}. The prepared sample has strong absorption in UV region and very weak absorption in near UV region. This absorption of light leads to optical excitation, so that electrons jump from valence band to conduction band, in which Mo has 4*d*-electrons, while W has 5*d*-electrons [20]. Many researchers explained that weak CTB is due to Eu-O, which is located in the region 250-350 nm. The CTB which is located in the region 350-400 nm due to Mo-O transition. It is also found that the steep fall of absorbance spectra around 400-450 nm is due to band gap transition, but not due to crystal defects in host lattice structure [21].

Morphological studies: From FESEM image, the sample of x = 0.12, consists of loosely packed structure of round shape grains with strong agglomerations' and the particle size ranging on average from 20-30 nm and the distance between particle

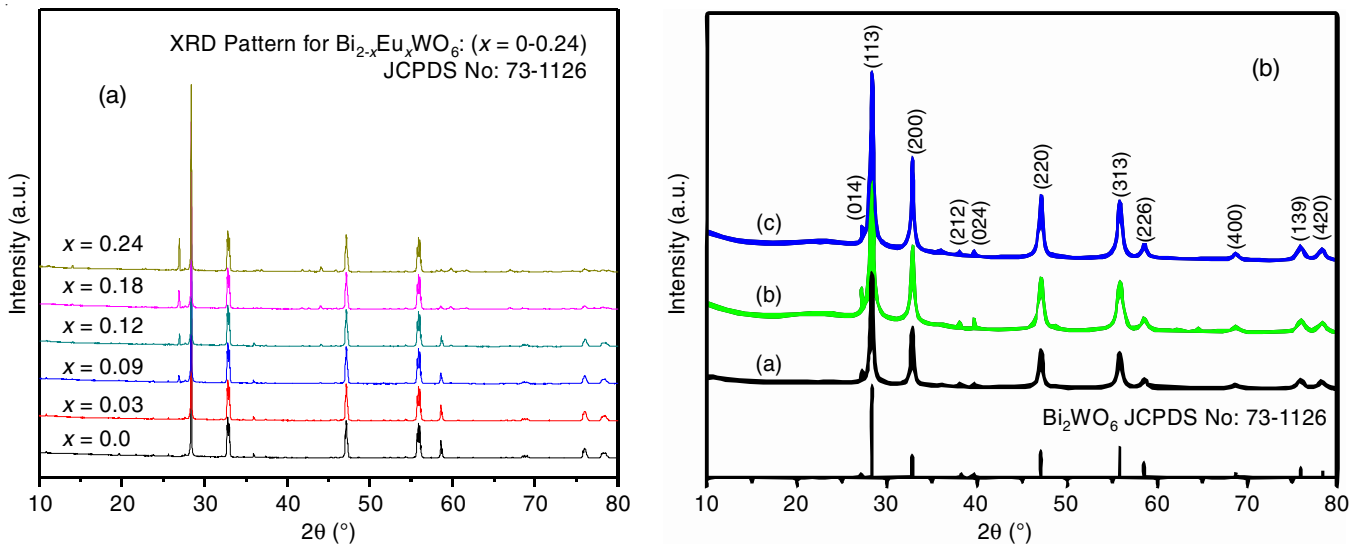

Fig. 1. XRD pattern for $Bi_{2-x}Eu_xWO_6$ at x = 0.0-0.24 of Eu^{3+} concentrations

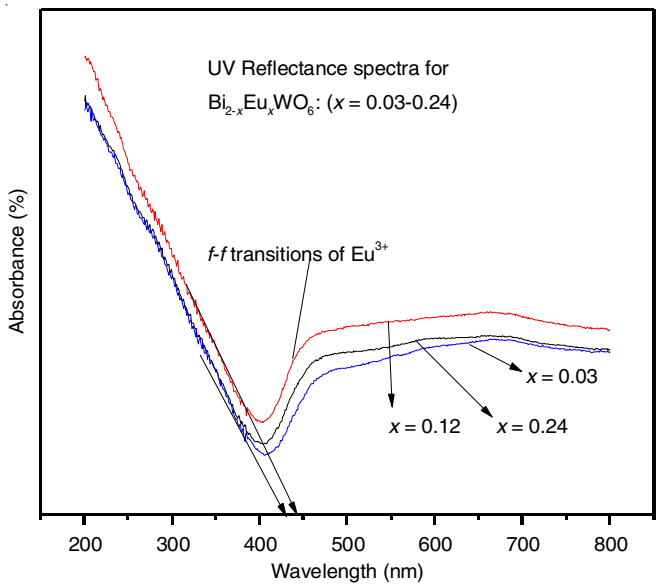

Fig. 2. UV-Vis reflectance spectra for $Bi_{2-x}Eu_xWO_6$ at x = 0.03-0.24 of Eu^{3+}concentrations

lies in between 100-200 nm. On other hand, many voids are appeared in the SEM image due to in adequate sintering temperature. However, it was observed that voids which enhances the luminescence properties of red phosphor. On the other hand, the prepared red phosphor's size lies in the range of 200 nm – 1 µm. Hence, the prepared sample also exhibits high luminescence as like commercial red phosphor and it can be used in luminescence, display devices and WLEDs. From Fig. 3, the prepared sample composition is seen in EDAX pattern. As a result, the stoichiometric percentage of elements in the EDAX data is almost equal to the elemental stoichiometry of the prepared phosphor sample.

Photoluminescence studies

Excitation spectra: Fig. 4a shows excitation spectra for $Bi_{2-x}Eu_xWO_6$, where the charge transfer band (CTB) lies in the range of 300-370 nm, which is due to W^{6+}-O and Eu^{3+}-O transitions [22]. In Fig. 4a, sample x = 0.12 shows a high intensity charge transfer band transition, which has comparatively less intensity than *f-f* transition. Moreover, the rest of all samples show low intensity charge transfer band transition than *f-f* transition. In addition, the *f-f* transitions are gradually increases with increase concentration and reaches maximum for x = 0.12 sample. Thereafter, the intensity of *f-f* transition is gradually decreases with the increase of concentrations *i.e.* (x = 0.15-0.24).

Hence, x = 0.12 concentrated sample is considered as the optimum concentration level for recording emission spectra of $Bi_{2-x}Eu_xWO_6$ at various wavelengths. So, it is concluded that charge transfer band indirectly helps the luminescent centre to emit high intensity transition. Moreover, diffuse reflectance spectra (DRS) supports the optimum concentration of x = 0.12, by showing the systematic red shift of absorption edge with increase concentration from x = 0.0-0.12. In this spectrum, the sharp peaks were appeared at 465 and 545 nm wavelengths and their corresponding transitions are $^7F_0$–$^5D_2$ and $^7F_0$–$^5D_1$, respectively. Out of these three peaks, relatively 465 nm wavelength peak has prominent absorption, which gives high intensity emission at 614 nm wavelength.

Emission spectra: Fig. 4b shows the emission spectra for compound $Bi_{2-x}Eu_xWO_6$ recorded at 465 nm excited wavelength. The main emission peaks lies in the range of 550-700 nm. The corresponding emission peaks are assigned as $^5D_0$–^7F_J (J = 0, 1, 2, 3). Among all four transitions $^5D_0$–$^7F_2$ transition shows highest intensity for the sample x = 0.12, due to the non-centro symmetric nature of Eu^{3+} in the host crystal lattice [23]. The other transitions at 595, 650, 700 nm are considered to be as moderate weak and very weak. The transition $^5D_0$–$^7F_2$ represents very good red light emission phosphor at 614 nm, which is supported by Li & Liu [24].

Sun *et al.* [25] and Blasse *et al.* [26] proposed an equation to calculate the critical transfer distance (R_c) between the two activator ions in the host crystal lattice. The equation given below as:

$$R_c = 2\left(\frac{3V}{4\pi X_c N}\right)^{1/3}$$

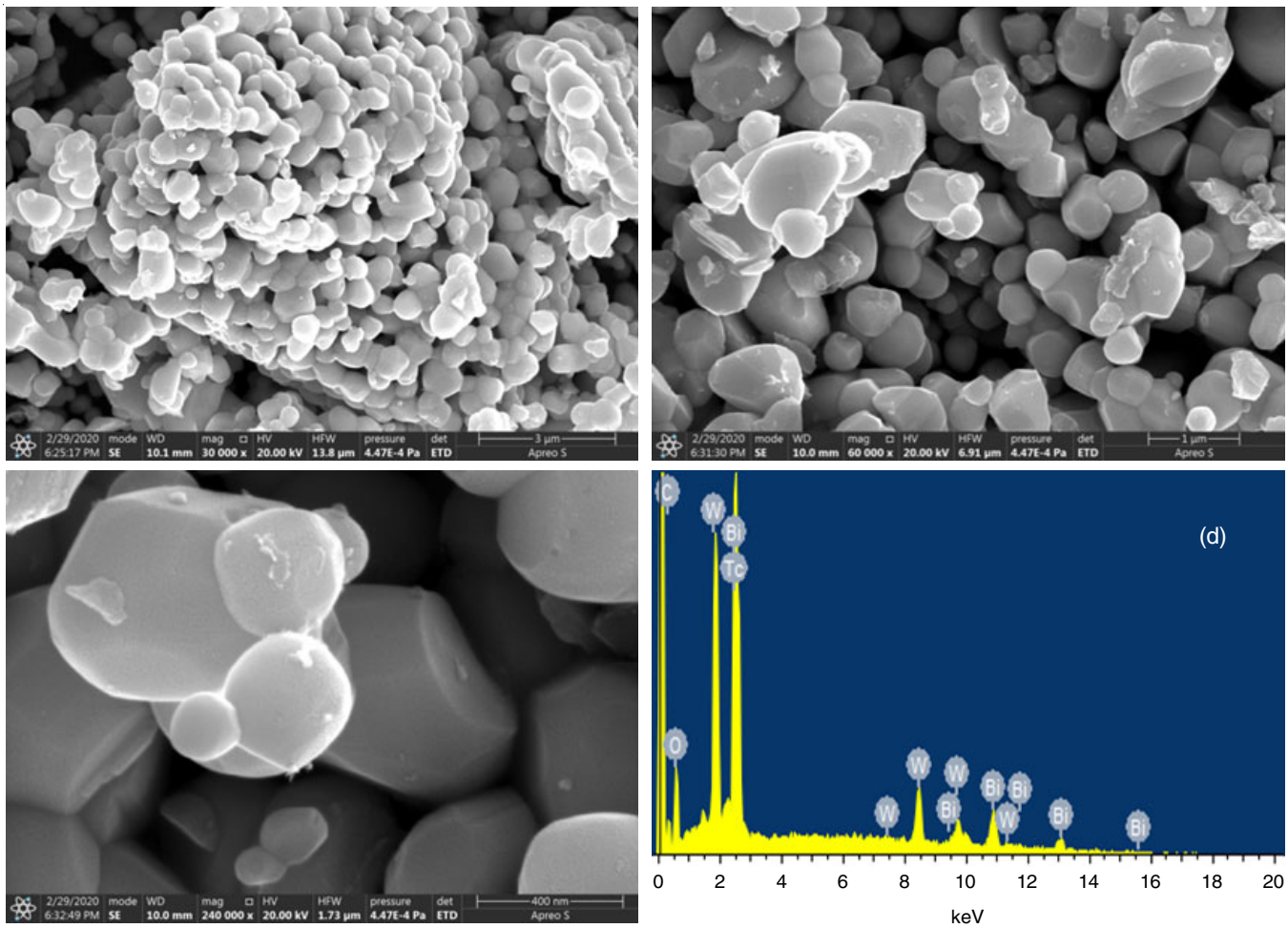

Fig. 3. SEM images of $Bi_{2-x}Eu_xWO_6$ at 400 nm, 10 μm and 1 μm. (d) EDAX pattern for $Bi_{2-x}Eu_xWO_6$

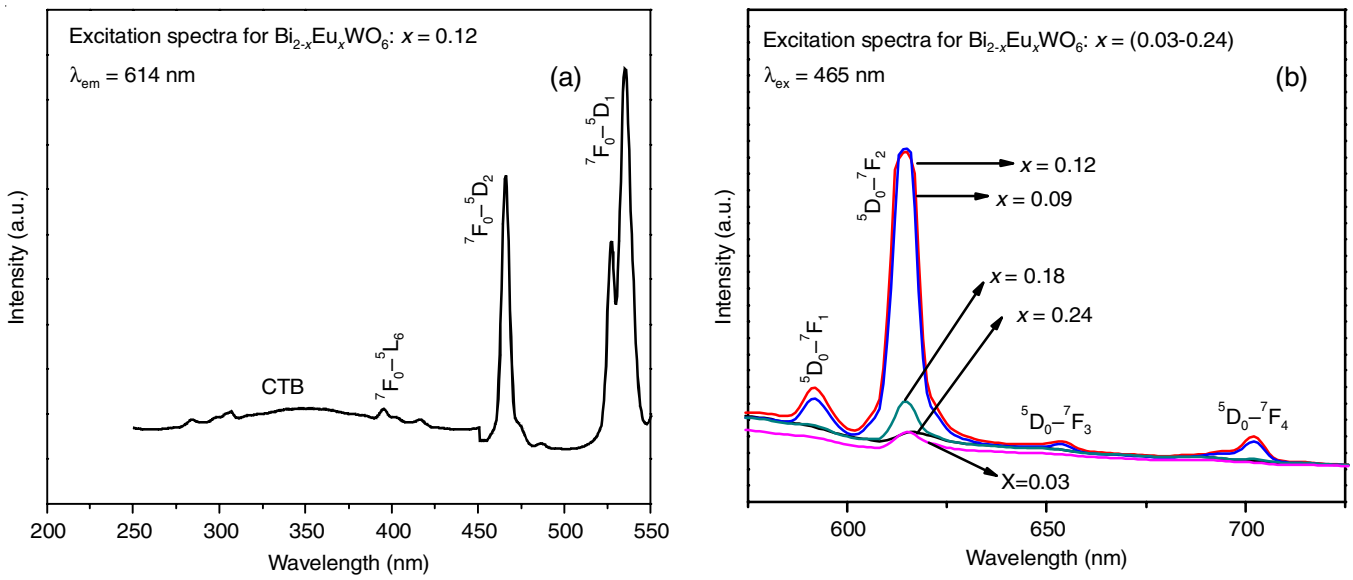

Fig. 4. Excitation spectra of (a) $Bi_{2-x}Eu_xWO_6$ at x = 0.12 obtained by monitoring 614 nm emission; (b) $Bi_{2-x}Eu_xWO_6$ for x = 0.03–0.24 obtained by exciting at 465 nm

where V is the volume of the unit cell, X_c is the atom fraction of Eu^{3+} activator in which the concentration quenching occurs and N represents the number of host cations in one-unit cell. So the unknown parameters for $Bi_{2-x}Eu_xWO_6$ are X_c = 0.12, V = 494.58.29, N = 4.0. Thus the calculated R_c value is 12.29 Å, which is greater than 5 Å, hence the energy transfer between

the activator ions is mostly associated with the multipolar interactions, radiation reabsorption. It also indicates that the multipolar–multipolar interaction is more dominant and results in the quenching of Eu^{3+} in the phosphors [27].

In addition to this, quenching depends mainly on the energy transfer between the ions in the host crystal lattice. But, the energy transfer depends on the distance between ions presented in the host crystal lattice. The distance of Eu^{3+}–Eu^{3+} ions varies in different layers of host material. However, ions Eu^{3+}–Eu^{3+} present in the same layer have very low range of distance than the ions present in the different layers of host crystal lattice. Similarly, the distance between Eu^{3+}–Eu^{3+} ions is very low along the *a*-axis, with comparative to the *b* and *c*-axis. Thus, it takes more energy transfer in the same layer along *a*-axis in the host crystal lattice. According to Dexter [28], the energy transfer easily takes place between the identical ions. In which one of the ions acts like sink due to its existence next to a defect.

CIE coordinates of phosphors: The prepared red phosphor chromaticity coordinators (*x*,*y*) have been measured using the CIE software (CIE 1931 XY.V.1.6.0.2) and the data is given in Table-1. The obtained results of chromaticity co-ordinators (*x*,*y*) are closed to the standard red phosphor, *i.e.* (0.67, 0.33). On the other hand, the sample with x = 0.12 concentrated sample shows very close to the chromaticity co-ordinators of the commercial standard red phosphor. In addition to this, the obtained coordinators are very close to the CIE edge in the CIE diagram (Fig. 5). It indicates that the luminescence intensity and colour purity of prepared phosphor can be optimized by increasing the concentration of Eu^{3+} dopants gradually.

By gradual increment of Eu^{3+} dopants into the host crystal lattice, the ratio of R/O increases and leads to destroy the symmetric nature of the prepared red phosphor. Hence, the red colour purity, emission intensity and the availability of different excitation chips can be optimized. Similarly, the colour tone of the prepared red phosphor changes with the increasing of Eu^{3+} ion concentration. It varies from yellowish orange to orange-reddish and finally turns to red colour tone. Once the colour tone is optimized, it can't be changed with the gradual increment of Eu^{3+} dopant concentration. The colour purity (CP) of the prepared sample can be measured with below equation [19,29]:

$$CP = \frac{\sqrt{(x - x_i)^2 + (y - y_i)^2}}{(x_d - x_i)^2 + (y_d - y_i)^2}$$

where (x,y) are the prepared sample coordinators, (X_d,Y_d) are the dominant wavelength co-ordinators and (X_i,Y_i) are the standard white light coordinators. For sample $Bi_{2-x}Eu_xWO_6$: Eu^{3+} (x = 0.12 concentration), the (*x*,*y*) is (0.6254,0.3746), (X_d,Y_d) is (0.66,0.31) and (X_i,Y_i) is (0.31,0.32). So from the equation the colour purity for the prepared sample is 92.5%, which shows the sample falls in the red region and also the CCT values are also lies around 1200-1900 K, for all the different concentrations of $Bi_{2-x}Eu_xWO_6$ for x = 0.03-0.24.

TABLE-1
CIE CO-ORDINATES OF $Bi_{2-x}Eu_xWO_6$ FOR (x = 0.03-0.24) FROM EMISSION SPECTRA EXCITED AT 465 nm

Sample	CIE x (465 nm)	CIE y (465 nm)	CCT (K)
$Bi_{1.97}Eu_{0.03}WO_6:Eu^{3+}$	0.5703	0.4296	1742
$Bi_{1.91}Eu_{0.09}WO_6:Eu^{3+}$	0.6167	0.3833	1285
$Bi_{1.88}Eu_{0.12}WO_6:Eu^{3+}$	0.6254	0.3746	1208
$Bi_{1.82}Eu_{0.18}WO_6:Eu^{3+}$	0.5864	0.4131	1644
$Bi_{1.79}Eu_{0.21}WO_6:Eu^{3+}$	0.5639	0.4358	1823
$Bi_{1.76}Eu_{0.24}WO_6:Eu^{3+}$	0.5592	0.4404	1886

Conclusion

A series of samples of composition $Bi_{2-x}Eu_xWO_6$ (x = 0.03-0.24) were prepared by a citrate-gel precursor method and all

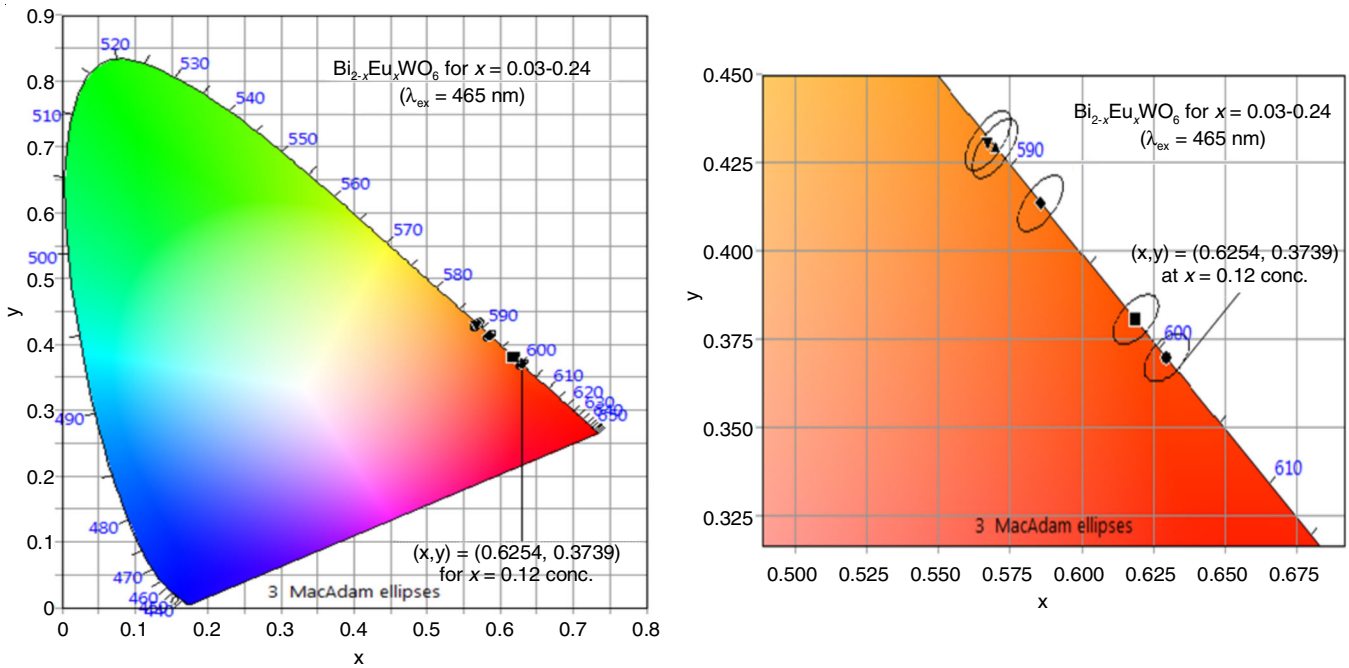

Fig. 5. CIE chromaticity coordinates of $Bi_{2-x}Eu_xWO_6$ for x = 0.03-0.24 (λ_{ex} = 465 nm)

of them crystallized in orthorhombic structure as confirmed by powder XRD. The morphology of samples is nearly spherical shape and size ranged from few nm to microns. The emission spectra recorded by exciting at 465 nm, showed the maximum intensity at 614 nm for $x = 0.12$ in the series of $Bi_{2-x}Eu_xWO_6$: Eu^{3+}. The colour purity and chromaticity coordinates were closed to standard red light in the CIE diagram and therefore, useful in WLEDs.

CONFLICT OF INTEREST

The authors declare that there is no conflict of interests regarding the publication of this article.

REFERENCES

1. Y.S. Hu, W.D. Zhuang, H.Q. Ye, S.S. Zhang, Y. Fang and X.W. Huang, *J. Lumin.*, **111**, 139 (2005); https://doi.org/10.1016/j.jlumin.2004.07.005
2. S.X. Yan, J.H. Zhang, X. Zhang, S.Z. Lu, X.G. Ren, Z.G. Nie and X. Wang, *J. Phys. Chem. C*, **111**, 13256 (2007); https://doi.org/10.1021/jp073991c
3. L. Chen, Y. Zhang, A. Luo, F. Liu, Y. Jiang, Q. Hu, S. Chen and R.-S. Liu, *Phys. Status Solidi Rapid Res. Lett.*, **6**, 321 (2012); https://doi.org/10.1002/pssr.201206234
4. Y.D. Huh, J.Y. Park, S.S. Kweon, J.H. Kim, J.G. Kim and Y.R. Do, *Bull. Korean Chem. Soc.*, **25**, 1585 (2004); https://doi.org/10.5012/bkcs.2004.25.10.1585
5. M. Thomas, P.P. Rao, S.P.K. Mahesh, L.S. Kumari and P. Koshy, *Phys. Status Solidi*, **208**, 2170 (2011); https://doi.org/10.1002/pssa.201026702
6. Z. Wang, H. Liang, J. Wang, M. Gong and Q. Su, *Appl. Phys. Lett.*, **89**, 071921 (2006); https://doi.org/10.1063/1.2335579
7. Z.L. Wang, H.B. Liang, M.L. Gong and Q. Su, *Electrochem. Solid-State Lett.*, **8**, H33 (2005); https://doi.org/10.1149/1.1865672
8. S. Li, X.T. Wei, K.M. Deng, X.N. Tian, Y.G. Qin, Y.H. Chen and M. Yin, *Curr. Appl. Phys.*, **13**, 1288 (2013); https://doi.org/10.1016/j.cap.2013.03.027
9. V. Pankratov, L. Grigorjeva, D. Millers, A.S. Voloshinovskii and S. Chernov, *J. Lumin.*, **94-95**, 427 (2001); https://doi.org/10.1016/S0022-2313(01)00326-X
10. K.V. Dabre, J.A. Wani, S.J. Dhoble, S.P. Lochab and A.S. Nakhate, *Phys. Status Solidi, B Basic Res.*, **258**, 2000442 (2021); https://doi.org/10.1002/pssb.202000442
11. C. Kodaira, H. Brito, O. Malta and O. Serra, *J. Lumin.*, **101**, 11 (2003); https://doi.org/10.1016/S0022-2313(02)00384-8
12. M. Nazarov, D. Jeon, J. Kang, E.J. Popovici, M. Zamoryanskaya, L.E. Muresan and B.S. Tsukerblat, *Solid State Commun.*, **131**, 307 (2004); https://doi.org/10.1016/j.ssc.2004.05.025
13. V. Mikhailik, H. Kraus, D. Wahl, M. Itoh, M. Koike and I. Bailiff, *Phys. Rev. B Condens. Matter Mater. Phys.*, **69**, 205110 (2004); https://doi.org/10.1103/PhysRevB.69.205110
14. R.B. Pode and S.J. Dhoble, *Phys. Status Solidi*, **203**, 571 (1997); https://doi.org/10.1002/1521-3951(199710)203:2<571::AID-PSSB571>3.0.CO;2-S
15. U. Kaufmann, M. Kunzer, K. Kohler, H. Obloh, W. Pletschen, P. Schlotter, J. Wagner, A. Ellens, W. Rossner and M. Kobusch, *Phys. Status Solidi*, **192**, 246 (2002); https://doi.org/10.1002/1521-396X(200208)192:2<246::AID-PSSA246>3.0.CO;2-I
16. L.M. Chen, Y.M. Long, Y.M. Qin and W.F. Li, *Mater. Lett.*, **102-103**, 59 (2013); https://doi.org/10.1016/j.matlet.2013.03.109
17. C.R. Reddy, C.V. Krishna, U.S.U. Thampy, Y.P. Reddy, P.S. Rao and R.V.S.S.N. Ravikumar, *Phys. Scr.*, **84**, 025602 (2011); https://doi.org/10.1088/0031-8949/84/02/025602
18. M. Guan, X. He, T. Shang, J. Sun and Q. Zhou, *Prog. Nat. Sci.*, **22**, 334 (2012); https://doi.org/10.1016/j.pnsc.2012.09.002
19. J. Zhang, B. Han, P. Li, J. Li and Y. Bian, *Opt. Spectrosc.*, **118**, 735 (2015); https://doi.org/10.1134/S0030400X15050082
20. Y. Liu, W. Luo, R. Li, G. Liu, M.R. Antonio and X. Chen, *J. Phys. Chem. C*, **112**, 686 (2008); https://doi.org/10.1021/jp077001z
21. S. Ye, C.H. Wang, Z.S. Liu, J. Lu and X.P. Jing, *Appl. Phys. B*, **91**, 551 (2008); https://doi.org/10.1007/s00340-008-3028-0
22. G. Blasse and B.C. Grabmaier, A General Introduction to Luminescent Materials, In: Luminescent Materials, Springer, Berlin, Heidelberg (1994).
23. C.C. Wu, K.B. Chen, C.S. Lee, T.M. Chen and B.M. Cheng, *Chem. Mater.*, **19**, 3278 (2007); https://doi.org/10.1021/cm061042a
24. Y. Li and X.H. Liu, *Opt. Mater.*, **42**, 303 (2015); https://doi.org/10.1016/j.optmat.2015.01.018
25. J.Y. Sun, J.H. Zeng, Y.N. Sun, J.C. Zhu and H.Y. Du, *Ceram. Int.*, **39**, 1097 (2013); https://doi.org/10.1016/j.ceramint.2012.07.032
26. G. Blasse, *Phys. Lett. A*, **28**, 444 (1968); https://doi.org/10.1016/0375-9601(68)90486-6
27. C. Yang, F. Wang, W. Li, J. Ou, C. Li and A. Amirfazli, *Appl. Phys., A Mater. Sci. Process.*, **122**, 1 (2016); https://doi.org/10.1007/s00339-015-9525-1
28. D.L. Dexter and J.H. Schulman, *J. Chem. Phys.*, **22**, 1063 (1954); https://doi.org/10.1063/1.1740265
29. G.F. Li, Y.G. Wei, Z.M. Li and G. Xu, *Opt. Mater.*, **66**, 253 (2017); https://doi.org/10.1016/j.optmat.2017.02.018